Particle-by-Particle Reconstruction of Ultrafiltration Cakes in 3D from Binarized TEM Images

Florent Bourgeois, Frédéric Courteille

DOI: 10.1002/ceat.201000097

Particle-by-Particle Reconstruction of Ultrafiltration Cakes in 3D from Binarized TEM Images

Transmission electron microscopy (TEM) imaging is one of the few techniques available for direct observation of the microstructure of ultrafiltration cakes. TEM images yield local microstructural information in the form of two-dimensional grayscale images of slices a few particle diameters in thickness. This work presents an innovative particle-by-particle reconstruction scheme for simulating ultrafiltration cake microstructure in three dimensions from TEM images. The scheme uses binarized TEM images, thereby permitting use of lesser-quality images. It is able to account for short- and long-range order within ultrafiltration cake structure by matching the morphology of simulated and measured microstructures at a number of resolutions and scales identifiable within the observed microstructure. In the end, simulated microstructures are intended for improving our understanding of the relationships between cake morphology, ultrafiltration performance, and operating conditions.

Keywords: 3D reconstruction, Cake microstructure, Multiresolution, Multiscale, Ultrafiltration

Florent Bourgeois[1]
Frédéric Courteille[1]

[1] University of Toulouse, Laboratoire de Génie Chimique, Toulouse Cedex 4, France.

1 Problem Statement

Water purification using ultrafiltration membranes is an industrial-scale process that replaces both coagulation and sand filtration. At present, stakes are high for increasing the cost-effectiveness of the process. One key dimension to this problem is the correlation between ultrafiltration efficiency (production rate and filtrate quality) and the microstructure of the cake, also known as the ultrafiltration cake, that forms on the membrane surface during the ultrafiltration process. As in other filtration processes, cake microstructure is a crucial element in this problem. But ultrafiltration differs from other filtration processes in that direct observation of the morphology of an ultrafiltration cake is particularly difficult. Because particles are nanosized, only a few techniques are available for capturing local information about the microstructure of ultrafiltration cakes. Amongst them, TEM imaging has been successfully used for direct observation of ultrafiltration cake microstructure [1]. The grayscale information from TEM images is potentially valuable for spatial reconstruction. However, it turns out that the quality of TEM images when imaging nanostructures is often insufficient for making quantitative use of the grayscale information. Hence, there is value in developing a reconstruction scheme that uses binarized TEM images only. Such images correspond to the projection of the particles captured by TEM images onto a plane situated anywhere inside the cake slice captured by the TEM scan. A typical TEM image and its binarized transform are shown in Fig. 1 for an ultrafiltration cake obtained using 26-nm monodispersed spherical particles. The thickness of the cake slice captured in this TEM image is 80 nm, which is typical of what can be expected from current TEM machines and sample preparation techniques.

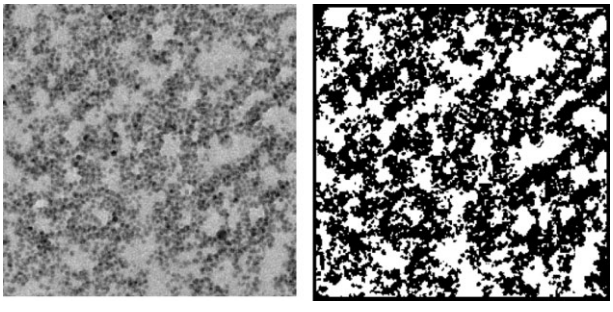

Figure 1. Original and binarized TEM image of an ultrafiltration cake (image size ≈ 1 μm^2).

Correspondence: Prof. F. Bourgeois (florent.bourgeois@ensiacet.fr), University of Toulouse, Laboratoire de Génie Chimique, 4, Allée Émile Monso, 31432 Toulouse Cedex 4, France.

2 3D Reconstruction Scheme

In order to reconstruct ultrafiltration cakes from cross-section images, several options can be selected. At one end of the spectrum of reconstruction solutions, one finds statistical models as described in references [2–5], for example. With the Cox process for instance, Jeulin and Moreau [6] were able to estimate the parameters of several Boolean processes which they combined to reconstruct microstructures with aggregates. In general, statistical models can be used provided particles are arranged according to some process whose spatial statistical properties can be extracted from morphological functions measured on 2D images. This approach is elegant and attractive, both computationally and analytically. At the other end of the spectrum, one may consider one of several reconstruction schemes that use numerical optimization algorithms. Examples of optimization reconstruction schemes can be found in references [7–10]. For example, Oberdisse et al. [9] have used the reverse Monte Carlo (RMC) technique for simulating fractal aggregates. Although they did not start from images, as they used small-angle neutron scattering (SANS) information instead, their procedure starts from a randomly formed aggregate, which they rearrange using the RMC algorithm until the SANS spectrum of the reconstructed aggregate matches the one measured. In principle, optimization techniques can be applied to structures larger than single aggregates. However, the task becomes more complex as the number of particles increases. Moreover, choosing the number of particles is a critical step with such reconstruction schemes as the reconstructed volume must be filled with particles before the start of the rearrangement process. The particle rearrangement algorithm is also computer intensive. However, there is no reason why such an approach could not be made to work satisfactorily.

The procedure developed in this paper sits somewhere between purely statistical and optimization approaches. The former was not selected on the basis that there is no evidence that ultrafiltration cakes conform to any particular statistical configuration. The authors avoided using the latter approach because they are designed to seek a global optimum, not one solution amongst many. Moreover, optimization schemes present foreseeable difficulties with simulating large volumes. The proposed reconstruction approach uses an incremental particle-by-particle reconstruction scheme of a cake slice, which corresponds to the volume captured by the TEM image. Adding particles one by one avoids having to specify the number of particles a priori and circumvents the difficult choice of this unknown. At every iteration, i.e., every time a new particle is added into the system, the point, $P(x, y, z)$, at which it is implanted is chosen such that it minimizes the difference between the specific surface area of the real microstructure and the specific surface area of the reconstructed microstructure at the current iteration with the new particle added at point P. In practice, the new particle can be positioned at random locations of two types. If the targeted specific surface area is less than that measured at the end of the previous particle addition step (see Fig. 2), the particle is positioned at a randomly chosen location such that its projected area does not overlap with that of other particles. Hence, it contributes its whole perimeter to the specific surface area. Otherwise, as shown in Fig. 3, it is positioned at a randomly chosen location such that its projected area overlaps with that of other particles, thereby contributing only marginally to the change in specific surface area.

The specific surface area can be calculated directly from the image by counting pixels that are located at the interface between the porous and solid phases. However, the function that is used in this work is the classical 2-point covariance function, S [2, 11, 12, 13], which is defined over the set of chords of length h. Not only is S a reliable means for calculating specific surface area from binary images [3, 11], but it also captures a

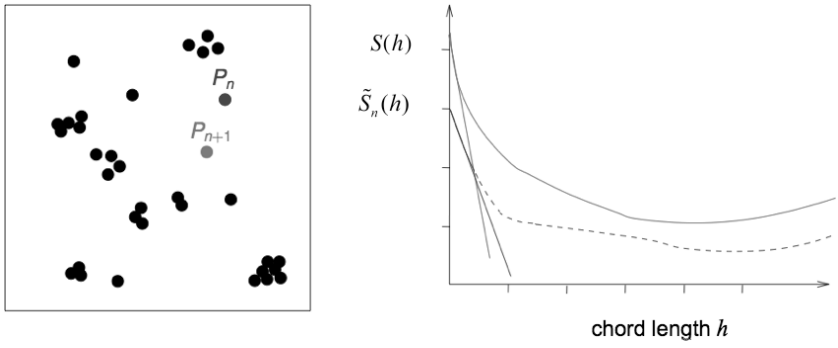

Figure 2. The targeted specific surface area is less than that measured at iteration n. Hence, particle P_{n+1} is positioned at iteration n+1 at random inside the reconstructed volume such that its projected area does not overlap with that of other particles. S and $\tilde{S}_n$ correspond to the two-point covariance function of the targeted image (solid line) and the reconstructed structure (dotted line) after n iterations, respectively.

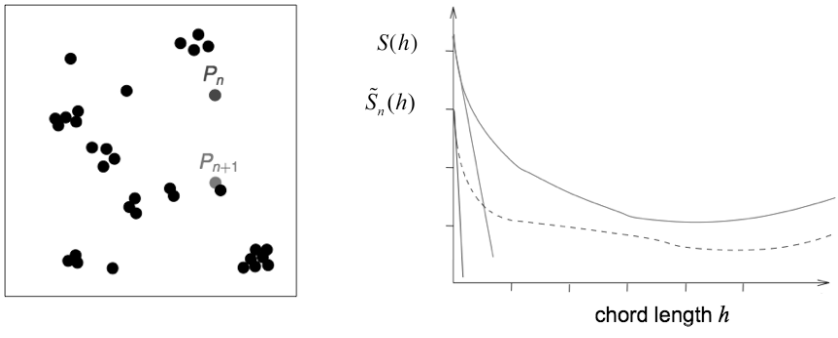

Figure 3. The targeted specific surface area is higher than that measured at iteration n. Hence, particle P_{n+1} is positioned at iteration n+1 at a position such that its projected area overlaps with that of other particles. S and $\tilde{S}_n$ correspond to the 2-point covariance function of the targeted image (solid line) and the reconstructed structure (dotted line) after n iterations, respectively.

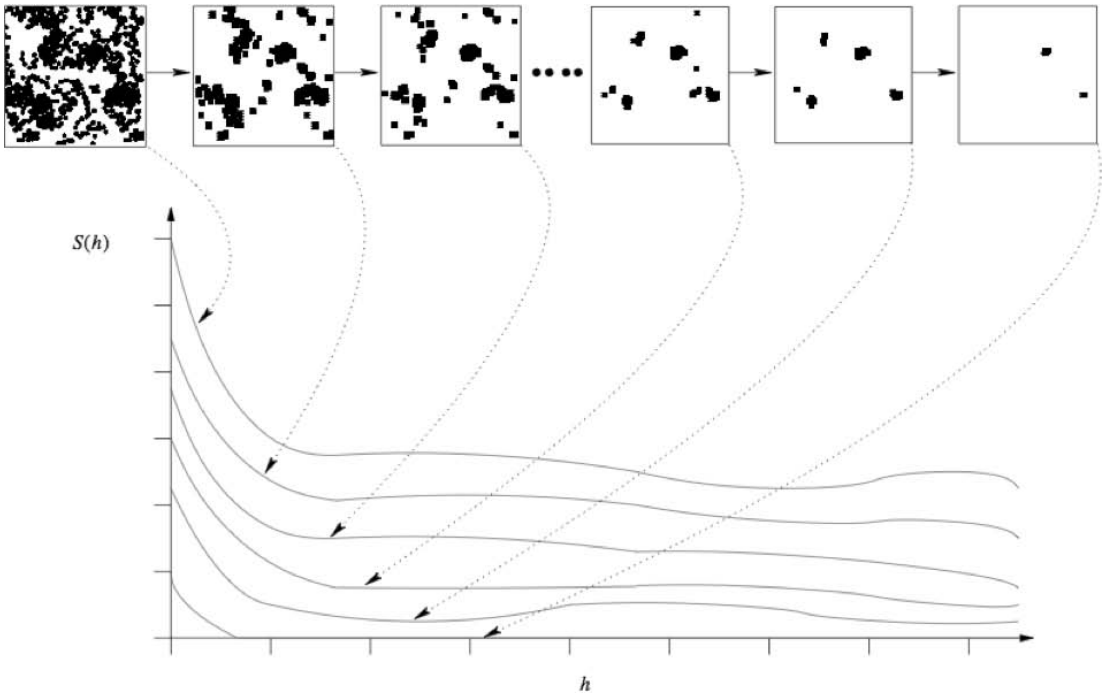

Figure 4. Illustration of the multiscale image analysis scheme.

meaningful short-range morphological signature of the texture. The authors have found that, despite the fact that the proposed reconstruction algorithm relies on matching the specific surface area only, the 2-point covariance function of the textures reconstructed with the proposed method matches that of the original textures over significant chord lengths. The reason for this interesting finding is believed to be the combination of the multiscale and multiresolution reconstruction scheme that is presented later, and the specified particle shape which constrains the 2-point covariance function significantly.

The next issue consists of capturing the multiscale nature of the texture from the image of the texture, from single particles to large aggregates. Quantification of the multiscale information of the texture is achieved in two successive steps, as described in Fig. 4: step one, a set of images of individual scales is generated by successive application of an erosion operator[1)]; step two, the 2-point covariance function is computed for each scale.

The multiscale texture simulation algorithm then simply consists of matching the 2-point covariance function at every individual scale, starting from the upper scale (rightmost image in Fig. 4) and moving to the left of Fig. 4 towards the lower scales. Addition of particles reduces the porosity of the image. Hence, the 2-point covariance function, *S(h)*, moves upward every time a particle is added to the system. Once the porosity of the current scale is matched, the algorithm uses the slope of the 2-point covariance function of the next scale as the next target for the particle-by-particle addition scheme presented earlier. This innovative particle-by-particle addition process gives an optimally-controlled growth of the reconstructed microstructure.

The scale-controlled microstructure reconstruction path followed by the proposed multiscale scheme was found to yield realistic porous media reconstructions, provided the microstructure did not exhibit too long a range order. In order to better match the observed microstructure over long ranges, multiresolution was added into the reconstruction scheme. A series of increasingly coarse resolutions, each one characterized by one image, are calculated by applying the dilation operator[1)] to the original binarized TEM image. Every image thus generated is analyzed by the multiscale analysis scheme, which identifies the scales within each resolution. Assuming the multiresolution analysis scheme identifies r resolutions and that the multiscale analysis scheme identifies s_i scales within resolution i, the reconstruction scheme is controlled by a total number of 2-point covariance functions equal to $\sum_{i=1}^{r} s_i$. The total number of resolutions and the number of scales within each resolution depend on the microstructure of the binarized TEM image.

The reconstruction scheme then takes the reverse path. It moves forward by reconstructing the microstructure from the highest resolution down to the lowest one, which is that of the binarized TEM image. The multiscale reconstruction process is used to simulate the texture at each resolution, as described earlier. Particles that are added into the reconstruction volume

1) Erosion is one of the two elementary operators in the area of mathematical morphology [2], the other being dilation. The basic effect of the operator is to erode away the boundaries of regions of foreground pixels (black pixels).

to simulate the texture at any given resolution correspond to the cake particles dilated by the same number of dilations that was used to generate the resolution in question. The positions available for adding particles at resolution n–1 is restricted to the particulate volume of the microstructure reconstructed at resolution n. It is this inter-resolution inclusion principle that gives the proposed reconstruction scheme the ability to match long-range textural order.

3 Results and Analysis

Firstly, the simulation algorithm was tested against images obtained from slices through an artificial cake generated using the physico-chemical model developed by Madeline et al. [1]. This is an ideal situation in that particles in the images are spherical and every spatial property is known for the particles inside the cake, making it possible to develop and fully test the validity of the reconstruction scheme.

Fig. 5 shows the results obtained when simulating the texture whose frame is bolded with the proposed algorithm. Fig. 5 was deliberately presented as a children's *Spot the difference* game, with the original cake slice image placed amongst 8 simulations. Should the bold frame be removed, it then becomes rather difficult to spot the original image in Fig. 5, thereby confirming the potential of the proposed 3D simulation technique for ultrafiltration cake slice simulation. We note, however, some differences with the reconstruction of the aggregates. The cause is an insufficient sampling of the larger particle aggregates in the original image, due to the fact that the technique used to generate the artificial ultrafiltration cake could only produce relatively small cake volumes.

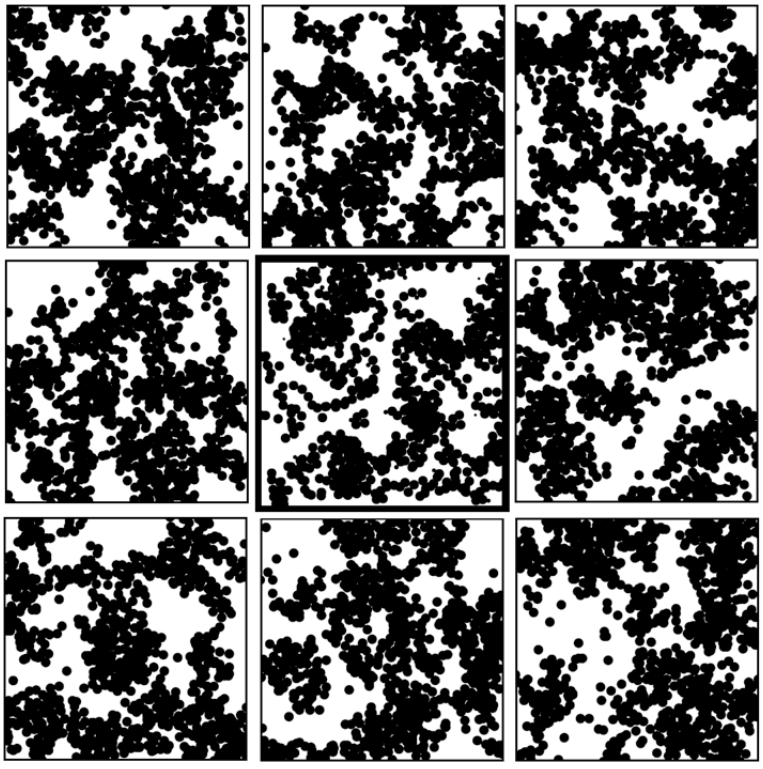

Figure 5. Projected image of the artificial ultrafiltration cake slice (bold frame) and 8 projected images of simulated slices using the proposed reconstruction method.

For the sake of illustration, Fig. 6 gives intermediate results of an ongoing particle-by-particle reconstruction at the final resolution, for which the target image is shown in the lower right corner. What is referred to as final resolution here corresponds to the lowest resolution, that is the resolution of the observed microstructure. The values at the bottom right corner indicate the number of particles that have been added into the reconstruction slice volume as reconstruction proceeds. One can readily see the progressive state of clustering of the particles, as they are being added into the volume restricted by the reconstruction at the previous resolution according to the scale-controlled reconstruction path.

The second application of the proposed method is the reconstruction of the binarized TEM image of a real ultrafiltration cake, which was presented in Fig. 1. Contrary to the artificial cake reconstructed in Figs. 5 and 6, the sampling of the aggregates is more satisfactory, as the field of view is large relative to the size of the largest aggregates. One reconstruction result is shown in Fig. 7, directly to the right of the original image. A notable difference with the previous ideal example is that particles no longer appear as spheres in the raw image. This is due to both the size of the particles (26-nm nominal diameter) and the binarization step applied to the grayscale TEM image. Nevertheless, the projected image of the simulated slice gives a satisfactory match to the original image. Moreover, as we hinted earlier, Fig. 7 confirms the match between simulated and measured 2-point covariance functions at a number of intermediate scales.

Visually, every reconstructed image is satisfactory. One observes that the simulation scheme recovers correctly both the void space and the state of particle aggregation. The state of aggregation is better recovered than with the artificial cake used earlier as the raw image provides a good sampling of the morphological features that correlate over long distances.

Quantitatively, the quality of the convergence was assessed using chi-square statistics, which showed equality between measured and reconstructed 2-point covariance functions at a confidence level greater than 95 %. In particular, the interfacial area was precisely matched, as confirmed by the match between the slopes of the 2-point covariance functions near the origin.

Fig. 8 gives a 3D view of one of the cake slices whose projection was shown in Fig. 7. The reconstruction scheme described here uses binarized TEM images only, which do not contain information that can be used directly to derive particle position in the vertical direction. Without additional constraint, the reconstruction algorithm yields a particle network that is looser than the real one. This problem is successfully overcome by using the

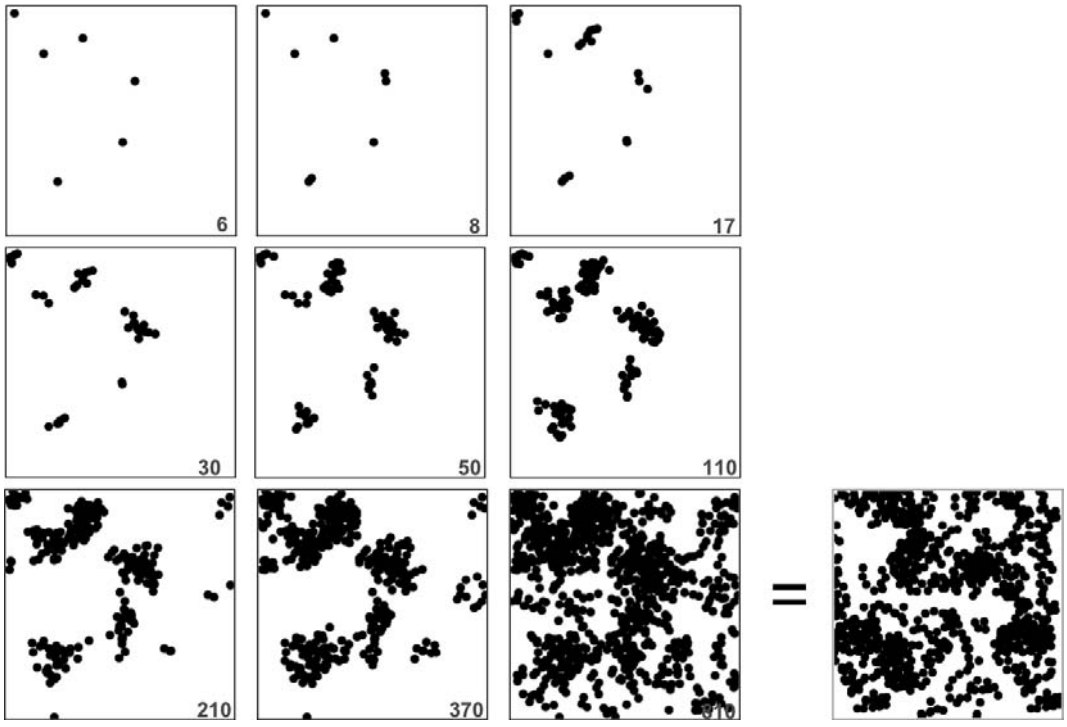

Figure 6. Illustrative example of the scale-controlled particle-by-particle addition scheme at the final resolution.

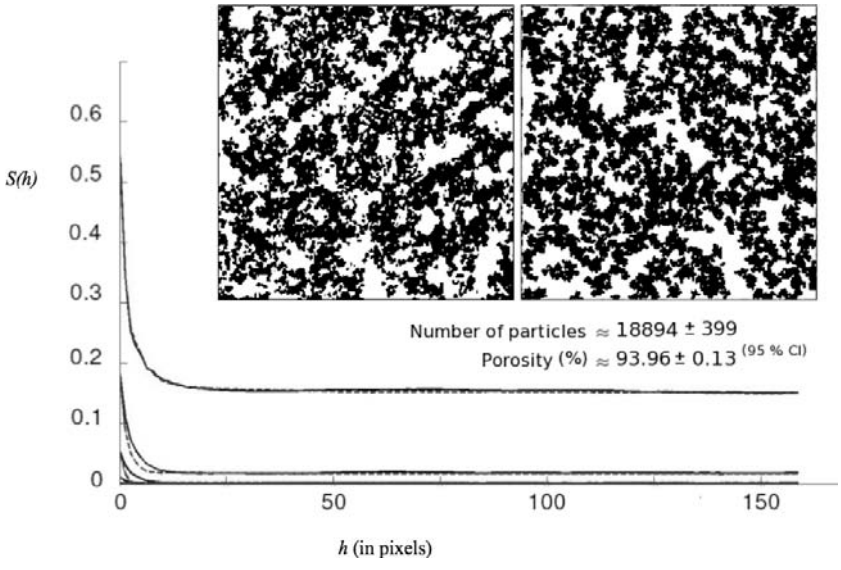

Figure 7. 3D simulation of a real ultrafiltration cake slice (original binarized TEM image to the left; simulated image to the right). Measured 2-point covariance functions are represented as a solid line, whereas simulated functions are shown as dotted lines. Confidence intervals are given for 300 simulations.

algorithm described above to position particles in the xy-plane and then selecting vertical positions that favor inter-particle contact in 3D where possible (i.e., when the projection of the particle is not isolated in the projected image of the slice under reconstruction). This constraint embeds the physics of particle deposition in an ultrafiltration cake, which dictates that particles must form a connected network. The authors have checked from artificial cakes (see earlier example illustrated in Fig. 6) where the number of particles that are implanted in the reconstructed volume is very close to the number of particles inside the original cake slice. One explanation is that ultrafiltration cakes are very dilute systems, so almost every particle inside a slice a few particle diameters in thickness will contribute something to the projected binary image of that slice. In other words, only very few particles can possibly hide directly behind others inside the thickness of the thin cake slice captured by TEM. Nevertheless, the reconstruction scheme presented in this paper does not yield the exact number of particles inside the slice, nor can it possibly "decide" what the best vertical position might be for each particle inside the reconstructed slice.

In the end, 3D reconstruction is intended for helping us to investigate and understand the relationships between cake morphology, ultrafiltration performance, and operating conditions. A 3D reconstructed porous cake can, for example, be input into transport codes as boundary conditions for calculating flow properties. Many publications have been written on investigation of fluid flow from porous media simulated in 3D.

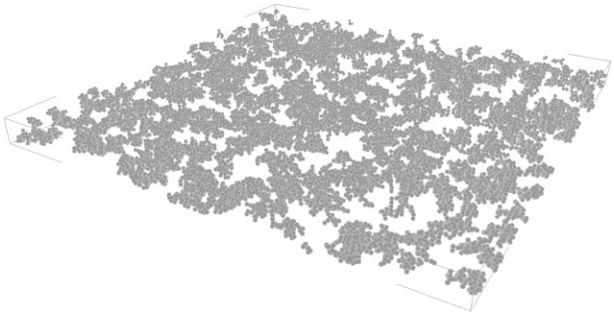

Figure 8. Example of a 3D ultrafiltration cake slice simulated with the proposed multiscale method.

For example, Adler et al. [14, 15] investigated the permeability of porous media from reconstructed porous media. Keehm et al. [16] applied the Lattice-Boltzmann technique, which is particularly relevant with complex porous media for simulation of 3D flow in reconstructed porous media. Many such examples can be found throughout the literature. It should be stressed that a major advantage of reconstructing 3D textures is that it permits generation of many different random realizations, thereby providing confidence intervals for any property that can be derived from microstructure simulations, either by simulation or from direct analysis of the reconstructed microstructures. For example, the 300 simulations from which one example was given in Figs. 7 and 8 gave the 3D porosity distribution shown in Fig. 9. This is a particularly important practical point as it is often the case that only one single ultrafiltration cake image is available for a given set of experimental conditions.

4 Conclusions and Perspectives

This article presented a new scheme for simulating ultrafiltration cakes from binarized TEM images. Such images can be obtained in practice even from poor-quality grayscale images: this makes the proposed approach particularly valuable for studying the morphology of nanostructures.

The originality of the proposed 3D simulation scheme is manifold. Firstly, the scheme uses a particle-by-particle addition process. Hence, the 3D simulation does not rely upon any assumption about the spatial statistics of the system and simulated volumes are not limited in size as with numerical optimization reconstruction schemes. Secondly, the proposed simulation scheme simulates multiscale textures successfully by matching the morphology of simulated and measured textures at every individual scale. The morphological properties of the texture at every scale, for any given resolution, are quantified using the 2-point covariance function. Because the scheme adds particles of a given shape and size distribution into the reconstruction volume, it is found that it is sufficient to match the y-intercept and the slope near the origin of the 2-point covariance function in order to obtain satisfactory 3D simulations. Thirdly, a multiresolution description of the microstructure is built into the scheme in order to describe long-range order. Overall, the proposed technique is quite straightforward to implement. Convincing simulation results were obtained with both ideal and real ultrafiltration cakes. It should be noted that such conditions correspond to images of thin slices of dilute cakes. Strictly speaking, the proposed scheme is applicable provided that all the particles present in the slice volume captured by TEM contribute in a measurable way to the image. If this condition is not met, as with thick and/or dense slices, the proposed reconstruction scheme should not be applied.

The proposed scheme is not generic. However, all things considered, it requires only a relatively small degree of tuning. Factors that are required include the erosion operator for multiscale analysis, the dilation operator for multiresolution analysis, the shape and size distribution of the elementary particles – which should correspond to the ultrafiltration cake particles – and a rule for positioning particles along the z-axis, since this information is not readily available in binarized TEM images.

Development of a generalized version of this 3D simulation algorithm that solves the problem of reconstructing a whole

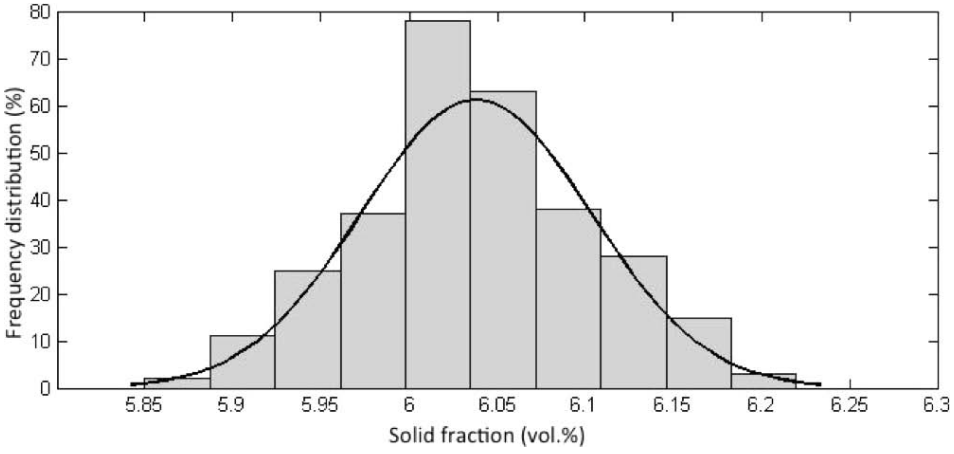

Figure 9. Example of the solidosity distribution of simulated ultrafiltration cake slices using the proposed reconstruction scheme.

cake from one or more TEM images is ongoing. The principle consists of using a moving reconstruction volume whose thickness equals that of the TEM image, centred on the vertical position of the particle that is added during the particle-by-particle addition reconstruction scheme. Hence, a volume larger than the simulated slice is built in the end, in such a way that every slice centred on every particle inside the system has a projected image whose 2-point covariance function matches the measured values. Using an elevation-invariant 2-point covariance function, or an elevation variant function, the technique is able to reconstruct not just one single cake slice, but a whole ultrafiltration cake. Moreover, the technique that is developed here with spheres can readily be applied using other particle shapes (e.g., polyhedra) and distributions of particle size. Hence, with such a technique, which is quite simple to implement, one should be able to simulate a wide variety of multiscale two-phase materials. It is worth noting that the 3D simulation technique presented here could also be applied to multi-phase systems, using inter-phase 2-point covariance functions.

References

[1] J. B. Madeline, *Langmuir* **2007**, *23 (4)*, 1645.
[2] J. P. Serra, *Image Analysis and Mathematical Morphology*, Academic Press **1982**.
[3] R. P. King, *Chem. Eng. J.* **1996**, *62*, 1.
[4] D. Jeulin, *Statistics and Computing* **2002**, *10*, 121.
[5] P.-S. Koutsourelakis, G. Deodatis, *J. Eng. Mech.* **2005**, *131 (4)*, 397.
[6] D. Jeulin, M. Moreau, in *Proc. ECS9*, Zakopane **2005**.
[7] C. L. Y. Yeong, S. Torquato, *Phys. Rev. E* **1998a**, *57*, 495.
[8] C. L. Y. Yeong, S. Torquato, *Phys. Rev. E* **1998b**, *58 (1)*, 224.
[9] J. Oberdisse, P. Hine, W. Pyckhout-Hintzen, *Soft Matter* **2007**, *3*, 476.
[10] X. Zhao, J. Yao, Y. Yi, *Transport in Porous Media* **2007**, *69*, 1.
[11] J. G. Berryman, *J. Appl. Phys.* **1985**, *57 (7)*, 2374.
[12] Y. Jiao, F. H. Stillinger, S. Torquato, *Phys. Rev. E* **2007**, *76*, 031110.
[13] Y. Jiao, F. H. Stillinger, S. Torquato, *Phys. Rev. E* **2008**, *77*, 031135.
[14] P. Adler, *Porous Media: Geometry and Transport*, Butterworth-Heinemann, Stoneham **1992**.
[15] S. Torquato, *Random Heterogeneous Materials: Microstructure and Macroscopic Properties*, Springer-Verlag, New York **2001**.
[16] Y. Keehm, T. Mukerji, A. Nur, *Geophys. Res. Lett.* **2004**, *31 (4)*, L04606.